Int. J. Devl Neuroscience 41 (2015) 115–122

Contents lists available at ScienceDirect

International Journal of Developmental Neuroscience

journal homepage: www.elsevier.com/locate/ijdevneu

A reliable and valid method for manual demarcation of hippocampal head, body, and tail

Ana M. Daugherty[a], Qijing Yu[a,b], Robert Flinn[a], Noa Ofen[a,c,*]

[a] Institute of Gerontology, Wayne State University, Detroit, MI 48202, USA
[b] Department of Psychology, Wayne State University, Detroit, MI 48202, USA
[c] Department of Pediatrics, School of Medicine, Wayne State University, Detroit, MI 48202, USA

ARTICLE INFO

Article history:
Received 19 December 2014
Received in revised form 2 February 2015
Accepted 3 February 2015
Available online 7 February 2015

Keywords:
Hippocampus
Manual tracing
Structural MRI
Brain development

ABSTRACT

There is a growing interest in characterizing functional specialization along the long axis of the hippocampus in humans. Variability in volumetry along the long axis of the hippocampus may be of functional relevance in human development, and in a number of clinical populations. However, there is a lack of consistent definitions for measurements of regional volumetry along the hippocampal long axis. Moreover, there is lack of consistent reliability standards of these measures. Here we describe a protocol for manual demarcation of hippocampal head, body, and tail. The definitions emphasize anatomical landmarks that agree with the extant literature and are visible in children and adults alike. Using this protocol we achieved high reliability of all volumetric measures. We further demonstrate that the protocol can be applied to T2-weighted images optimized for high-resolution scanning of the hippocampus, as well as a more standard T1-weighted image sequence. Third, the protocol is sensitive to detect individual differences in subregion volumes in normally developing children ($N = 81$; ages 8–25 years). This protocol may be of use for researchers studying the hippocampus across the lifespan and in diverse clinical populations.

1. Introduction

The hippocampus (Hc)[1] is a complex structure composed of several functional circuits (Duvernoy, 2005) that support complex functions of memory (Scoville and Milner, 1957; Tulving and Markowitsch, 1998; Aggleton, 2012). Recently, there has been an increased interest in quantification of subcomponents of the Hc formation in an effort to better understand the diverse functionality of the structure. To this end, researchers have turned their attention to the study of Hc subregions that span its long, anterior–posterior axis (Bouchard et al., 2008; Malykhin et al., 2010), or the Hc head, body, and tail. Based upon the functional projections of the Hc formation to the rest of the brain, the anterior–posterior subregions may support different functionality (Moser and Moser, 1998; Aggleton, 2012). Given the growing focus on a possible differential relation between Hc subregion volumetry and differences in developmental profiles, it is crucial that investigators use reliable and valid measurement methods. Although several researchers have published with their own procedures (e.g., Bouchard et al., 2008; Malykhin et al., 2010), a detailed description of a delineation method with demonstrated reliability and validity has not been shown before. Here, we present a protocol for manual demarcation of Hc subregions that meets this need.

Converging evidence from human and animal studies suggests different specialization of regions along the long axis of the Hc. Regions of the hippocampal long axis differ in gene expression (Strange et al., 2014) and project to different cortical and subcortical regions (Moser and Moser, 1998; Aggleton, 2012). (See Poppenk et al. (2013) for a schematic diagram of anterior–posterior hippocampal connectivity with the brain.) The regions spanning the Hc long axis may be differentially vulnerable to pathology and risk for clinical memory impairment, such as in post-traumatic stress disorder (Bonne et al., 2008), dementia and Alzheimer's disease (Gordon et al., 2013). Moreover, both structural (Maguire et al., 2000; Poppenk and Moscovitch, 2011) and functional (Chua et al., 2007; Giovanello et al., 2009; Poppenk and Moscovitch, 2011) differences account for variability in distinct aspects of human memory (Bannerman et al., 2004; Poppenk et al., 2013; Strange et al., 2014). Indeed, the anterior–posterior subregions may follow different developmental trajectories across the lifespan that mirror the development of specialized memory functions. Although

* Corresponding author at: Institute of Gerontology, Wayne State University, 87 E. Ferry Street, 257 Knapp Bldg., Detroit, MI 48202, USA. Tel.: +1 313 664 2643.
E-mail address: noa.ofen@wayne.edu (N. Ofen).

[1] Hc – hippocampus; ICC – intra-class correlation coefficient; PD-TSE – proton-density weighted turbo spin echo sequence; MPRAGE – magnetization prepared rapid gradient echo.

http://dx.doi.org/10.1016/j.ijdevneu.2015.02.001
0736-5748/

Hc volume is thought to be stable starting at the age of 4 years old (Gogtay et al., 2006; Mattai et al., 2011; Sullivan et al., 2011; Lin et al., 2013), the evidence regarding developmental differences along the long axis is mixed. One cross-sectional study of normal development reports larger anterior Hc volume in children 8–11 years old as compared to young adults (DeMaster et al., 2014), whereas others do not find differences in sub-regional volume (Lin et al., 2013). In the course of adult aging, advanced age is associated with smaller total Hc volume and some findings suggest greater age differences in anterior Hc regions (Watson et al., 1997; Chen et al., 2010), however, this localized effect is inconsistent across studies (Kalpouzos et al., 2009).

Taken together, the evidence suggests that anterior–posterior subregions of the Hc may be associated with specific cognitive functions, follow different developmental trajectories, and may be differentially vulnerable to pathology. Thus, quantifying individual differences in the structural integrity of Hc subregions may help explain the neural underpinnings of memory function across the lifespan, and its aberration in disease. Yet the extant evidence has two major limitations that greatly complicate interpretation. First, there are inconsistent measurement definitions for the anatomical subregions; and second, perhaps more critically, there is an inconsistent standard of measurement reliability for all regions, which is the initial barrier to valid measurement (Carmines and Zeller, 1979). Differential reliability of measures across regions taints claims of regional specificity in volumetric effects. With the intent to study development of Hc subregions and individual differences therein, a reliable and valid measurement method is necessary.

Here, we present a protocol for Hc subregional volumetry that meets this need. The definitions of Hc head, body, and tail emphasize anatomical landmarks that can be visualized on MRI, with which we demonstrate high intra- and inter-rater reliability with intra-class correlation [ICC(3) and ICC(2)] formulas (Shrout and Fleiss, 1979). In addition to demonstrating reliability, we aimed to validate the method by demonstrating measurement invariance across different MR image contrasts, and by reproducing reports of individual differences in Hc head, body, and tail that differentially correlate with age.

2. Method

2.1. Participants

All participants ($N = 81$; 42 females) were healthy, typically developing children and adults, ages 8–25 years ($M = 15.69$, SD = 5.02). Participants were recruited from the Metro Detroit region and met the following criteria for enrollment: reported no neurological injury, psychiatric disorders, or learning disabilities; born full-term; right-hand dominant; spoke English as a native language; and had no contraindications to MRI. Age-based standardized IQ scores (Kaufmann Brief Intelligence Test, KBIT–2) of the whole sample indicated average intelligence ($M = 108.14$, SD = 12.42), and IQ did not differ by age ($r = -0.06$, $p = 0.59$) or between sexes ($t(79) = 1.23$, $p = 0.22$).

From this sample, a subset was randomly selected to represent the broader age range for reliability procedures. The initial reliability procedures on the T2-weighted images used a set of $N = 12$ (ages 10–23 years), and the comparison of T2- to T1-weighted images used $N = 10$ (ages 10–23 years). Analysis of age differences in subregion volumes included the entire sample. In addition to the sample of 81, 7 participants (ages 15–23 years) were scanned but excluded as multivariate outliers that biased analyses, and 1 additional scan for a child was not sampled due to excessive motion. The 8 cases that were omitted from analyses did not differ from the retained sample in age ($t(87) = -1.93$, $p = 0.06$) or IQ ($t(87) = -1.15$, $p = 0.25$).

2.2. MR image acquisition

MRI data were collected in a 3 Tesla Siemens Verio (Siemens Medical AG, Erlangen, Germany) full body scanner with a 32-channel head coil at Harper Hospital Imaging Center, Wayne State University (Detroit, MI). The manual tracing protocol for Hc head, body, and tail measurements was developed based on a T2-weighted high-resolution proton density-weighted turbo spin echo (PD-TSE) sequence that was adapted from Bender et al. (2013). Images were acquired in the coronal plane perpendicular to the long axis of the Hc with the following parameters: voxel size = $0.42 \times 0.42 \times 2\,mm^3$ (30 slices); echo time = 17 ms; repetition time = 7150 ms; flip angle = 120°; pixel bandwidth = 96 Hz/pixel; limited field of view = 280×512 mm.

In addition to the high-resolution Hc sequence, a T1-weighted magnetization prepared rapid gradient echo (MPRAGE) sequence was collected for intracranial volume measurements and validation of the Hc head, body, and tail boundary definitions across imaging modalities. The T1 MPRAGE was acquired in the coronal plane perpendicular to the anterior–posterior commissures with the following parameters: interpolated voxel size 0.5 mm × 0.5 mm × 1.0 mm; echo time = 4.26 ms; repetition time = 2200 ms; inversion time = 1200 ms; flip angle = 9.0°; pixel bandwidth = 130Hx/pixel; GRAPPA acceleration factor PE = 2.

2.3. Protocol for reliable manual tracing of Hc head, body, and tail

Anatomical definitions for Hc head, body, and tail measurements were developed within our lab following atlases (e.g, (Duvernoy, 2005) and recommendations from procedures in the extant literature (Poppenk et al., 2013). Thus, Hc subregion boundaries were defined by anatomical landmarks and notable features of Hc morpometry. Definitions were determined to allow for reliable measurement of subregion volumes and emphasized valid representation of the neuroanatomay. Definitions were originally developed for manual demarcation on the T2-weighted high-resolution hippocampal MRI, on which reliability was initially established. Following the initial reliability assessment, the same definitions were applied to T1 MPRAGE images as an additional test of measurement invariance as evidence for validity.

The range of measurements was defined by anatomical landmarks that were present in all participants, and allowed to account for differences in Hc length that may vary by age (Insausti et al., 2010) or individual differences in head placement within the scanner. The most anterior slice was identified by visualization of the mammilary bodies and the range extended posterior until the pulvinar nucleus was no longer visualized and the body of the fornix was present. Measurements in both hemispheres began on the same anterior slice, but subsequent transitions between subregions and the last posterior slice were free to vary between hemispheres. See Fig. 1 for an example of demarcation.

2.3.1. Hc head

The range of the Hc head began on the most anterior slice and ended posterior to the uncal sulcus, when the digitations were no longer visualized. The anterior range was truncated to allow for separation of the amygdala from the Hc, which is similar to other procedures of total Hc volumetry (Raz et al., 2004). The lateral boundary was the temporal horn of the lateral ventricle; the medial boundary was the ventricle space and the entorhinal cortex. The boundary between the subiculum and entorhinal cortex was determined as a horizontal line projecting from the most medial aspect of the parahippocampal gyrus white matter to the ventricle.

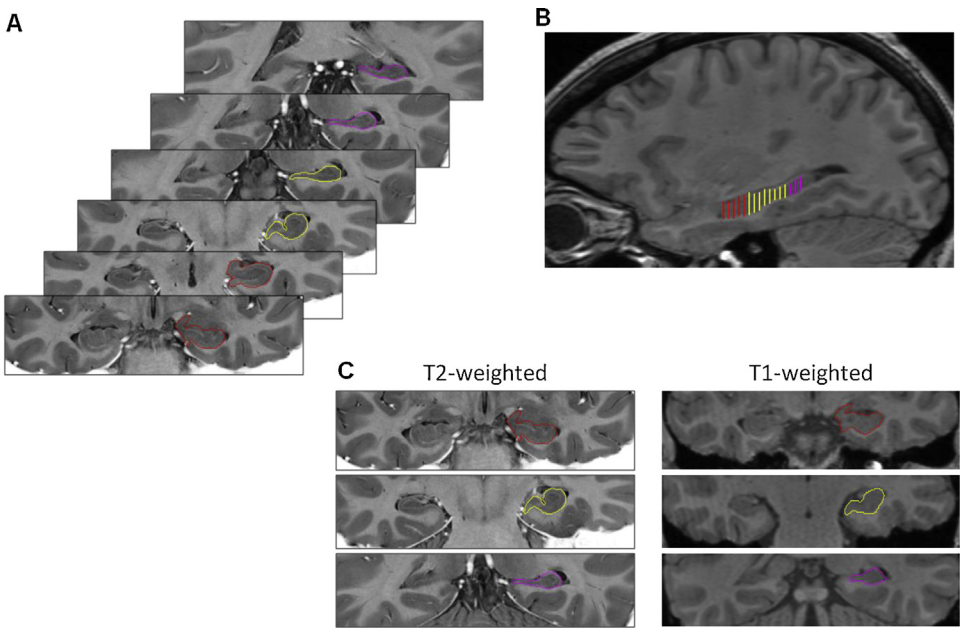

Fig. 1. Example hippocampal head, body, and tail demarcations. (A) Representative slices of hippocampal head, body, and tail traced on T2-weighted images, with $0.4 \times 0.4\,mm^2$ in-plane resolution and 2 mm slice thickness. Image intensity was inverted. Not all slices of the traced range are shown. Head – red; body – yellow; tail – purple. (B) Sagittal view of the hippocampus on a T1-weighted image ($0.5\,mm^3$) that has been aligned to be perpendicular to the long axis of the hippocampus. The range of hippocampal head, body, and tail measurements are shown along the long axis. (C) A comparison of representative hippocampal head, body, and tail tracings on T2-weighted and T1-weighted images. (For interpretation of the references to color in this figure legend, the reader is referred to the web version of this article.)

2.3.2. Hc body

The range of the Hc body began posterior to the head and ended when the fimbria fornix was visualized posterior to the pulvinar nucleus. The boundaries were defined the same as the head: the lateral ventricle for the lateral and medial boundaries, and a horizontal line defining the boundary between subiculum and parahippocampal gyrus cortex. When visualized, the choroid plexus and fimbria were excluded.

2.3.3. Hc tail

The range of the Hc tail extended from the end of the body to the last posterior slice. The boundary definitions were similar to that of head and body, except for the medial boundary between Hc and surrounding cortex, which was determined as a difference in morphometry visualized as a notch between the tapering Hc complex and the widening of the cortex on the dorsal parahippocampal gyrus. The fimbria fornix was excluded.

On the T2-weighted images with 2 mm slice thickness, the range included 15–17 contiguous slices: Hc head on 3–5 slices, the Hc body on 8–10 slices, and the Hc tail on 2–3 slices. Accommodating individual variability in anatomy and head placement in the scanner, this is approximately 30% of the entire range labeled as head, body 50%, and tail 20%. These definitions agree with suggested anatomical landmarks (Duvernoy, 2005), as well as percentage-based rules (Chen et al., 2010). Total Hc volume was measured as the sum of the subregions, which closely agrees with other procedures of total Hc volumetry (Raz et al., 2004). All images used in this study were processed with Analyze v11.0 software (Mayo Clinic, Rochester, MN) and manual demarcations were made using a stylus on a 21 in. digitizing tablet (Wacom Cintiq).

2.4. Additional procedures for demarcation on the T2-weighted high-resolution images

The T2-weighted images were magnified by a factor of two and intensities were inverted to mimic a T1-weighted inversion recovery sequence, which when visualizing the anatomy was more intuitive to the raters. Head, body, and tail measurements from the T2-weighted high-resolution images were taken from contiguous slices (2 mm slice thickness).

2.5. Additional procedures for demarcation on T1-weighted MPRAGE images

Prior to manual demarcation, the T1 MPRAGE was resliced to have a $0.5\,mm^3$ isotropic voxel, and realigned perpendicular to the long axis of the Hc, while aligning the anterior–posterior commissures using Analyze v11.0 software (Mayo Clinic, Rochester, MN). Differences in head tilt and yaw were manually corrected. The same anatomical definitions were applied when demarcating the T1 MPRAGE image sets, tracing every fourth slice (approximating the 2 mm slice thickness of the T2-weighted images), which was accounted for in volume calculations. There is little consequence to accuracy and reliability of volumetry at this sampling density as compared to measuring from every 0.5 mm slice (Eritaia et al., 2000).

2.6. Intracranial volumetry and regional volume correction

For the purpose of volume correction, intracranial volume (ICV) was manually measured from the T1 MPRAGE image sets. Prior to measurements, the $0.5\,mm^3$ isotropic T1 MPRAGE was manually aligned to the anterior–posterior commissures, and corrected for differences in head tilt and yaw. ICV was demarcated in the axial plane following procedures described in Raz et al. (2004). ICV was measured on every 20th slice for a total of 10 slices, beginning at the most dorsal slice on which brain tissue was visualized and extending ventrally. Five independent raters made measurements with high reliability: ICC(2) = 0.99.

Hc head, body, and tail volumes were calculated as the sum area across slices. For measurements from the T1 MPRAGE, the sum area was corrected for the slices that were not measured. Lateral and total subregion volumes were corrected for differences in ICV via analysis of covariance (Jack et al., 1989): $\text{volume}_{adj} = \text{volume}_i - b$

($ICV_i - ICV_{mean}$), where i denotes a measurement for an individual, b is the unstandardized coefficient of whole sample volume regressed on ICV, and ICV_{mean} is the sample mean. Although age correlates with ICV in this sample ($r = 0.58$, $p < 0.001$), the slope of regional volumes regressed on ICV was similar between child, adolescent, and adult age groups: all $F(1, 77) < 3.19$, $p > 0.08$. Therefore, the assumption of homogeneous slopes across age groups was met and the same correction was applied to the whole sample.

2.7. Reliability procedures

Prior to whole sample data collection, reliability for each region was confirmed via measurements from the T2-weighted high-resolution sequence. To demonstrate agreement between raters (A.M.D. & R.W.F.), a sub-set of 12 cases were demarcated and measurements were compared with an intra-class correlation coefficient formula assuming random raters, ICC(2) (Shrout and Fleiss, 1979). In addition, intra-rater reliability was confirmed for a single rater (A.M.D.) measuring the same set of 12 cases after a 2-week delay, ICC(3) (Shrout and Fleiss, 1979). For both reliability assessments, we employed a high standard of at least 0.85 for measurements from each hemisphere, and 0.90 for sum total measurement of each region.

2.8. Validating definitions of Hc head, body, tail volumetry from T1 MPRAGE images

Many laboratories collect T1-weighted structural images that are not optimized to show fine structures in the Hc that can be seen clearly on T2-weighted high-resolution images. Although a T1 MPRAGE sequence commonly has lower in-plane resolution (e.g., $1 \times 1\,mm^2$) than the customized T2-weighted ($0.4 \times 0.4\,mm^2$ as described above), the landmarks used to define the head, body, and tail measurements can still be visualized and be used to produce reliable measurements. For the purpose of demonstrating the applicability of our protocol to typical T1-weighted MPRAGE images, we confirmed reliability of our protocol when comparing measurements between the T2 high-resolution and T1 MPRAGE sequences. To do so, a reliable rater (A.M.D.) repeated head, body, and tail measurements in a sub-set of cases ($N = 10$) that also had a T1 MPRAGE image set. The rater was blind to the prior T2-weighted image tracing (more than 1 year had passed since viewing the T2 image sets), and intra-rater consistency was confirmed with ICC(3) (Shrout and Fleiss, 1979). The same standards of reliability were used: minimum ICC(3) of 0.85 for measurements of each hemisphere, and 0.90 for sum total of each region.

2.9. Analysis of individual differences in hippocampal subregion volumes

As an additional effort to validate our procedures for head, body, and tail measurement, we tested for individual differences in regional volumes that may differentially correlate with age. To do so, volumes that were adjusted for ICV were entered into a 3 (region) × 2 (hemisphere) repeated-measure general linear model (GLM). Age (continuous measure centered at the sample mean) and sex were entered as covariates. A significant age × region interaction effect was further explored with post-hoc univariate GLMs to determine the nature of differential age effects between regions. Prior to analysis, univariate outliers were winsorized, and to avoid spurious effects due to small sample size, all models were bootstrapped with bias-correction (5000 draws of the original sample; Hayes and Scharkow, 2013) to produce 95% confidence intervals (CI). Further, head, body, and tail volumes were regressed on age to calculate unstandardized residuals as a measurement of individual differences that were unrelated to age, and we tested for regional differences therein. Finally, as a confirmatory analysis, we tested for age differences in total Hc volume – measurements summed across regions – in a GLM framework, treating hemisphere as a 2-level repeated measure.

3. Results

3.1. Measurement reliability from T2-weighted images

Reliability was confirmed for all regional measures between raters in a sub-set of 12 cases. See Table 1 for a report of all reliability statistics. Agreement between raters was high for all regions, exceeding 0.90 for all measures, except for the right Hc body that was ICC(2) = 0.89, which still met our standard for reliability. Moreover, the same rater confirmed high internal consistency following a delay of 2 weeks: all ICC(3) > 0.91.

3.2. Measurement invariance across scan types: reliability between T2- and T1-weighted images

The same reliable rater repeated measurements in a sub-set of cases ($N = 10$) to compare volumes extracted from the T2-weighted images to those from the T1-weighted image sets. Similar volumes were produced and had high internal consistency: all ICC(3) ≥ 0.87 (see Table 1). Therefore, the same anatomical landmarks can be visualized on T1- and T2-weighted images to produce similar volume measurements.

Table 1
Estimates of reliability of Hc subregion volumes from the T2-weighted high-resolution and T1 MPRAGE images.

Region		T2-weighted images		Comparison of measures (T2- vs T1-weighted images)
		Between raters, ICC(2)	Within rater, ICC(3)	Within rater, ICC(3)
Head				
	Left	0.99	0.96	0.95
	Right	0.99	0.93	0.99
	Total	0.99	0.94	0.98
Body				
	Left	0.95	0.98	0.95
	Right	0.89	0.95	0.98
	Total	0.95	0.99	0.98
Tail				
	Left	0.95	0.92	0.87
	Right	0.92	0.91	0.93
	Total	0.95	0.92	0.93

Note: ICC – intra-class correlation coefficient (Shrout and Fleiss, 1979).

3.3. Individual differences in regional volumes

We first tested individual differences in regional volumes with respect to age. Age differences in regional volumes (adjusted for ICV) were estimated in a 3 (region) × 2 (hemisphere) repeated measure GLM. Because there was no difference in volumes between hemispheres ($F(1, 78) = 1.60$, $p = 0.21$), nor differential age effects between hemispheres ($F(1, 78) = 0.01$, $p = 0.91$), only total volumes summed across hemispheres were included in analyses of age effects by region. In the full sample, ages 8–25 years, age was unrelated to volumes of the Hc head, body, and tail ($F(1, 78) = 0.70$, $p = 0.41$) and age-effects did not differ by region (age × region $F(2, 77) = 0.75$, $p = 0.48$). This may be in part due to a large amount of variability in measurements in young adults in this sample. When the analysis of age effects was limited to participants age 8–18 years ($N = 59$), the age × region interaction was a non-significant trend: $F(2, 53) = 2.68$, $p = 0.07$. Exploring this effect further, older age was associated with smaller Hc head volume ($\beta = -42.49$, $p = 0.02$; 95% CI -76.61/-8.36), but not with volumes of Hc body ($\beta = -8.24$, $p = 0.55$; 95% CI -35.68/20.72) or tail ($\beta = -2.16$, $p = 0.71$; 95% CI -13.33/9.87; see Fig. 2). Finally, sex was entered as a covariate in all models, but there were no sex differences in regional volume ($F(1, 78) = 1.67$, $p = 0.20$), or differential effects between regions (sex × region interaction, $F(2, 77) = 0.81$, $p = 0.45$).

Accounting for the effects of age and sex, there remained a large degree of variability in Hc head ($R^2 = 0.07$), body ($R^2 = 0.001$), and tail ($R^2 = 0.05$) volumes to suggest additional factors to explain individual differences in regional volumetry. By residualizing regional volumes on age, we examined the amount of remaining variability in each region in the full sample. The remaining variability unrelated to age was larger in the Hc head than in the body ($F(80, 80) = 1.61$, $p = 0.04$), and variability in both these regions was larger than that in the tail ($F(80, 80) = 8.28$ and 5.16, $ps < 0.001$, respectively). Therefore, additional factors that explain individual differences in volume across the three regions may be different. The individual variability throughout childhood can be seen in Fig. 2 that depicts the associations between age (8–18 years) and regional volumes.

Although there is evidence of age-related differences in Hc head, total hippocampal volume was not related to age in the selected sample age 8–18 years ($F(1, 56) = 2.23$, $p = 0.14$), or in the full sample age 8–25 years ($F(1, 78) = 1.40$, $p = 0.24$).

4. Discussion

Our main goal in this paper is to present a protocol for reliable and valid quantification of Hc head, body and, tail volumetry. We developed the protocol using anatomical landmarks consistent with the extant literature, and achieved high reliability for measurements in all regions. We demonstrated that, using these landmarks, reliable measures of Hc head, body, and tail volumes can be taken from T2-weighted images optimized for high-resolution scanning of the hippocampal formation, as well as from T1-weighted images with lower resolution that is more commonly used in neuroimaging studies. By confirming similar volumetric measurements from both image types, we demonstrate a form of measurement invariance as evidence for the validity of the Hc subregion measures. Second to this, we offered convergent findings of individual differences in regional volumes, which age partially accounted for only in the Hc head. Taken together, our manual method provides reliable and valid measures of hippocampal subregional volumes. Further, adopting this method will facilitate consolidation of findings across laboratories to inform our understanding of structural differences and possible functional specialization along the Hc anterior–posterior axis in typical and atypical development.

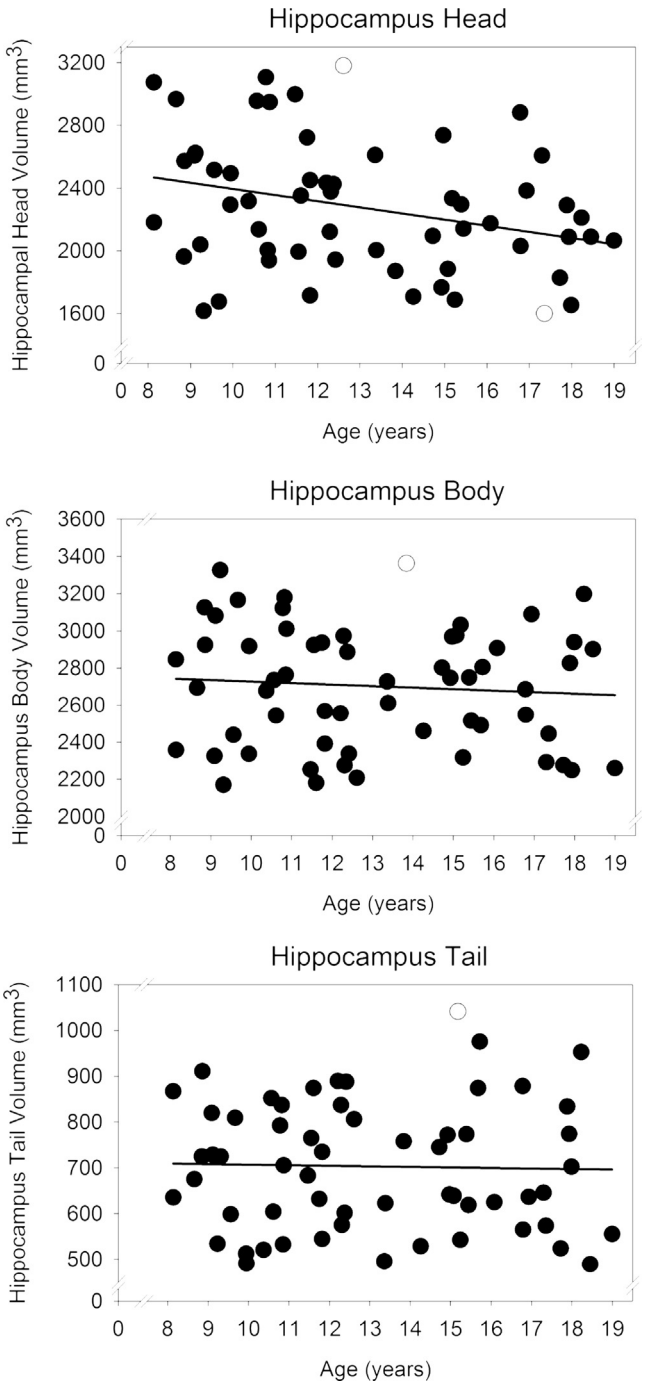

Fig. 2. Age differences in hippocampal head, body, and tail volumes in a sample selected to be age 8–18 years. A trend for regional differences in age effects ($F(2, 53) = 2.68$, $p = 0.07$) was identified in the selected sample to be age 8–18 years, but not in the total sample ages 8–25 years. Age-related differences from 8–18 years in the hippocampal head were significant ($p = 0.02$), but there were no effects in the body ($p = 0.55$) or tail ($p = 0.71$). Measurements were made from the T2-weighted high-resolution images. Regional volumes were corrected for intracranial volume (see Section 2 for details). Gray circles represent data points that were winsorized.

The anterior–posterior subregions appear to have a degree of specialization that is otherwise lost when measuring the whole Hc proper. Animal studies of gene expression demonstrate multiple domains along the hippocampal long axis, which often exhibit sharply demarcated borders (Strange et al., 2014). Different functional projections from the subregions to cortex and subcortical nuclei may underscore the functional specialization of the long axis (Moser and Moser, 1998; Aggleton, 2012), particularly as it per-

tains to memory functions. In humans, both structural (Maguire et al., 2000; Poppenk and Moscovitch, 2011) and functional (Chua et al., 2007; Giovanello et al., 2009; Poppenk and Moscovitch, 2011) variability in anterior–posterior regions account differentially for variability in memory function.

The precise nature of anterior–posterior functional specialization, however, remains unclear. Some researchers suggest anterior regions have specialized emotional and reward motivation functions in memory (Bannerman et al., 2004; Fanselow and Dong, 2010; Murty et al., 2010; Strange et al., 2014), however others identify similar correlations with posterior regions (Shafer and Dolcos, 2012; Dolcos et al., 2013). A popular hypothesis has been that posterior regions have unique spatial memory and navigation functions (Ryan et al., 2010; Woollett and Maguire, 2012), yet there is an evidenced role for anterior regions in recognition of relative spatial landmarks (Ekstrom et al., 2011; Morgan et al., 2011). Still others posit that anterior–posterior function may be organized on a scale of detail and flexibility in mnemonic processing – posterior regions are linked to detailed representations whereas anterior regions represent a gist of an experience rather than its details (Poppenk et al., 2013). The complexity of evidence for functional specialization further underscores the importance of characterizing the hippocampal anterior–posterior subregions with a robust method.

Variability in anterior–posterior Hc volumetry may be a meaningful predictor of cognitive outcomes across the lifespan under typical and atypical conditions. For example, adolescents who were born premature have smaller posterior Hc volumes as compared to full-term counterparts, and this accounts for worse verbal learning (Gimenez et al., 2004). Patients with post-traumatic stress disorder have smaller total Hc volume compared to their healthy counterparts, but critically, greater differences are observed in posterior regions (Bonne et al., 2008). Further, total hippocampal volumes are smaller in schizophrenic patients (Adriano et al., 2012), and neurons are smaller particularly in posterior regions in post-mortem comparisons to healthy brains (Benes et al., 1991) although a localized difference in volume has not been found in vivo (Weiss et al., 2005). In contrast, patients with multiple sclerosis (Longoni et al., 2013) and Alzheimer's disease (Gordon et al., 2013) also have smaller total Hc volume as compared to healthy adults, but in these populations greater differences are observed in anterior regions. However, when considering similar pathologies, reports of differential anterior–posterior effects are inconsistent. For example, when compared to controls, adults suspected to be in prodromal stages of Alzheimer's disease had smaller Hc head and tail volumes (Pluta et al., 2012), whereas another study reported smaller Hc head and body volumes in pre-symptomatic mild cognitive impairment (Martin et al., 2010). In future research, employing a similar measurement protocol with acceptable reliability will facilitate more meaningful comparisons across studies of different pathology and between studies of typical and atypical development.

As demonstrated, the protocol we present here may be employed across laboratories that use different image types. This is largely accomplished by using anatomical landmarks to define Hc head, body, and tail. Extant methods used in the investigation of anterior–posterior subregion volumetry can be broadly classified into two groups: landmark-based and percentile-based rules. For landmark-based rules, the recent review by Poppenk et al. (2013) suggests that the uncal apex is a valid landmark to distinguish the anterior–posterior subdivisions (Weiss et al., 2005), or the head and body (Malykhin et al., 2007; Martin et al., 2010; Yushkevich et al., 2010, Gordon et al., 2013; Widjaja et al., 2014), which is in agreement with anatomical atlases (e.g., Duvernoy, 2005). It also agrees with the coordinate-based rule in neuroimaging studies using standard atlases (e.g., MNI coordinate space, left: $y = -21$ mm, right: $y = -20$ mm, Poppenk et al. (2013); left: $y = -20$ mm, right: $y = -18$ mm, DeMaster and Ghetti, (2013)). Although fewer studies go on to segment the tail from the body, presentation of the fornix has been a common landmark (Pruessner et al., 2001; Ariza et al., 2006; Maller et al., 2006; Malykhin et al., 2007; Martin et al., 2010; Gordon et al., 2013; Widjaja et al., 2014). This landmak is in agreement with authoritative atlases (Duvernoy, 2005) and also corresponds to a coordinate-based rule in a neuroimaging study using a standard atlas (e.g., MNI coordinate space, left: $y = -36$ mm, right: $y = -34$ mm, DeMaster and Ghetti, (2013). Our protocol is consistent with these landmarks and has demonstrated high measurement reliability.

We made efforts to also determine our definitions in comparison to an alternate approach to landmark-based rules that segments the regions based upon percentage of Hc length. Assuming the full length of the Hc is labeled, the segmentation of head as 30–35%, body as 45%, and tail as the remaining 20–25% (Chen et al., 2010) appears to match well with the landmark definitions. Although there have been other definitions employed – e.g., 35%, 35%, and 30% (Echavarri et al., 2011), and 25%, 50%, and 25% (Maguire et al., 2000; Driscoll, 2003) for head, body, and tail, respectively. Differences in percentage-based definitions between studies may be a consequence of differences in imaging parameters and protocol for head placement in the scanner. The use of landmark-based definitions partially alleviates this concern, as visualization of common anatomical features is less susceptible to interference from differential head placement and can accommodate individual differences in Hc morphometry and length.

Regardless of the definitions used to delineate the anterior–posterior subregions, any method used must be demonstrated to be reliable before it can be tested for validity. For if a measurement is inconsistent, then the accuracy of its representation cannot be reasonably assessed (Carmines and Zeller, 1979). An inconsistent standard of reliability complicates the interpretation of unique regional effects, which may be an artifice of regional differences in the degree of error in measurements. The majority of manual or semi-automated procedures reported in the extant literature are accompanied by a minimum ICC value for reliability of all measurements. While a minimum reliability is acceptable to demonstrate overall consistency, it is difficult to determine if regions vary in their degree of consistency when claiming region-specific effects. An ICC (Shrout and Fleiss, 1979) exceeding 0.90 for total volume summed across hemispheres is a good standard of reliability, but not all studies meet this standard (e.g., Bouchard et al., 2008) and others use less appropriate methods to assess volumetric reliability (e.g., Weiss et al., 2005).

Measurements gained by using semi-automated brain segmentation tools with minimal human operator intervention, such as Freesurfer or voxel-based morphometry, can have high reproducibility, and thereby high internal consistency. However, typically these tools have not been validated against the gold standard of volumetry: manual demarcation with equally high internal consistency. Indeed, a recent report demonstrates systematic age bias in assessing hippocampal volumetry between younger and older adults (Wenger et al., 2014), and the validity of automated methods with respect to manual demarcation in children was never tested. Moreover, methods that localize functional activation to a portion of the Hc cannot assess reliability of subregion definitions the same way, and faced with this predicament, many researchers do not report the definitions used when labeling an effect as anterior or posterior Hc (e.g., Giovanello et al., 2009). The common label but inconsistent definitions of these subregions, compounded by inconsistent standards of reliability, undermine the validity of inferences from the standing evidence.

The protocol we present here can address these concerns. In addition to measurement reliability, we demonstrated that the same definitions can be used to produce similar estimates of volume from T2- and T1-weighted images. This determination of

measurement invariance across image types makes the protocol easily applied to other neuroimaging studies, including applying the definitions in functional imaging.

Further, measurements with these definitions are sensitive to capturing individual variability in regional volumes. Similar to other reports (DeMaster et al., 2014), age was negatively correlated with Hc head volume in the selected sample of participants age 8–18 years, however we did not find age differences in Hc body or tail volume. Although we partially replicate age differences in the Hc head that have been reported before (DeMaster et al., 2014), we did not find any evidence for subregional differences in volume between sexes (e.g., Gogtay et al., 2006). Absolute sex group differences were likely reduced by the correction of the subregion volumes for intracranial volume, which was necessary to remove the bias of sexual dimorphism in head size (Sgouros et al., 1999) from our analysis of age differences. Further, due to the limitation of the cross-sectional design that cannot accurately approximate individual differences in change (Lindenberger et al., 2011), we could not effectively test possible sex differences in the developmental trajectories of these regions (e.g., Gogtay et al., 2006; Bramen et al., 2011). Indeed, we found that age and sex accounted for a small portion of the individual differences in hippocampal subregion volumes. Pronounced individual differences throughout childhood and young adulthood suggest additional factors that may shape individual developmental trajectories. This intriguing finding warrants additional study. Applying the same method in future studies of typical and atypical development will provide greater insight into hippocampal structure and function.

The basis of variability in subregional volumes is unknown. Volumetry is a crude proxy of the underlying cytoarchitecture and microstructure that can only be assessed at a far finer resolution. Volumetry measures from MRI are sensitive to changes in neuropil (Qiu et al., 2013) and variability in myelination (Courchesne et al., 2000). Indeed, myelination of the medial temporal lobe during childhood can contribute to variability in MRI volumetry (Schneider and Vergesslich, 2007) and may partially account for the individual differences we report here. However, the possible differential representation of myelin along the longitudinal axis during childhood development is currently unknown.

In addition to myelin, the crude measures of subregion volumes may be capturing individual variability in the Hc subfields. The medial-lateral axis of the Hc is divided into cytoarchitectonically-distinct subfields, for which there is growing evidence of differential development (Daugherty et al., under review-a) and differential cognitive correlates (Bender et al., 2013; Daugherty et al., under review-b); also see (Krogsrud et al., 2014; Lee et al., 2014; Tamnes et al., 2014). The subfields are present throughout the long axis, and the contribution of age effects in specific subfields to variability in gross anterior–posterior volumetry is unknown. Nonetheless, there is initial evidence for differential effects of age in both the anterior–posterior and medial-lateral axis of the Hc. Because the method for head, body and tail volumetry was developed for T2-weighted high-resolution images, on which Hc subfields can also be reliably demarcated, in the future we will attempt to consolidate these effects into a cohesive model of hippocampal development. It is our hope that the use of reliable and valid measurement of anterior–posterior Hc volumetry will further our understanding of typical development and the etiology of certain clinical conditions.

5. Conclusions

We present a protocol for reliable measurement of subregions spanning the hippocampal anterior–posterior axis. We further validated this method by demonstrating similar measurements across MR image types and by replicating reports of individual variability in regional volumes that differentially correlates with age during childhood development. Future research may identify additional factors that contribute to individual variability and determine cognitive correlates that are unique to each Hc subregion. Reliable methods for assessing regional volumetry are crucial in determining whether variability in Hc subregion structural integrity have developmental and clinical relevancy.

Acknowledgements

The work presented here was partially supported by funding from the Institute of Gerontology at Wayne State University and a Graduate Research Award to NO. We thank Raphael Serota, Amanda Hardwick, Carson Miller and David Brush for help with data collection, and Mayu Nishimura and Naftali Raz for constructive discussions.

References

Adriano, F., Caltagirone, C., Spalletta, G., 2012. Hippocampal volume reduction in first-episode and chronic schizophrenia: a review and meta-analysis. Neuroscientist 18, 180–200.
Aggleton, J.P., 2012. Multiple anatomical systems embedded within the primate medial temporal lobe: implications for hippocampal function. Neurosci. Biobehav. Rev. 36, 1579–1596.
Ariza, M., Serra-Grabulosa, J.M., Junque, C., Ramirez, B., Mataro, M., Poca, A., Bargallo, N., Sahuquillo, J., 2006. Hippocampal head atrophy after traumatic brain injury. Neuropsychologia 44, 1956–1961.
Bannerman, D.M., Rawlins, J.N., McHugh, S.B., Deacon, R.M., Yee, B.K., Bast, T., Zhang, W.N., Pothuizen, H.H., Feldon, J., 2004. Regional dissociations within the hippocampus—memory and anxiety. Neurosci Biobehav Rev 28, 273–283.
Bender, A.R., Daugherty, A.M., Raz, N., 2013. Vascular risk moderates associations between hippocampal subfield volumes and memory. J. Cognit. Neurosci. 25, 1851–1862.
Benes, F.M., Sorensen, I., Bird, E.D., 1991. Reduced neuronal size in posterior hippocampus of schizophrenic patients. Schizophrenia Bull. 17, 597–608.
Bonne, O., Vythilingam, M., Inagaki, M., Wood, S., Neumeister, A., Nugent, A.C., Snow, J., Luckenbaugh, D.A., Bain, E.E., Drevets, W.C., Charney, D.S., 2008. Reduced posterior hippocampal volume in posttraumatic stress disorder. J. Clin. Psychiatry 69, 1087–1091.
Bouchard, T.P., Malykhin, N., Martin, W.R., Hanstock, C.C., Emery, D.J., Fisher, N.J., Camicioli, R.M., 2008. Age and dementia-associated atrophy predominates in the hippocampal head and amygdala in Parkinson's disease. Neurobiol. Aging 29, 1027–1039.
Bramen, J.E., Hranilovich, J.A., Dahl, R.E., Forbes, E.E., Chen, J., Toga, A.W., Dinov, I.D., Worthman, C.M., Sowell, E.R., 2011. Puberty influences medial temporal lobe and cortical gray matter maturation differently in boys than girls matched for sexual maturity. Cereb. Cortex 21, 636–646.
Carmines, E.G., Zeller, R.A., 1979. Reliability and validity assessment. In: In: Quantitative Applications in the Social Sciences. Sage Publications, Thousand Oaks, CA, pp. 14–15.
Chen, K.H., Chuah, L.Y., Sim, S.K., Chee, M.W., 2010. Hippocampal region-specific contributions to memory performance in normal elderly. Brain Cognit. 72, 400–407.
Chua, E.F., Schacter, D.L., Rand-Giovannetti, E., Sperling, R.A., 2007. Evidence for a specific role of the anterior hippocampal region in successful associative encoding. Hippocampus 17, 1071–1080.
Courchesne, E., Chisum, H.J., Townsend, J., Cowles, A., Covington, J., Egaas, B., Harwood, M., Hinds, S., Press, G.A., 2000. Normal brain development and aging: quantitative analysis at in vivo MR imaging in healthy volunteers. Radiology 216, 672–682.
Daugherty, A.M., Bender, A.R., Raz, N., Ofen, N., under review-a. Age differences in hippocampal subfield volumes from childhood to late adulthood.
Daugherty, A.M., Bender, A.R., Yuan, P., Raz, N., under review-b. Changes in search path complexity and length during learning of a virtual water maze: age differences and differential associations with hippocampal subfields volumes.
DeMaster, D., Pathman, T., Lee, J.K., Ghetti, S., 2014. Structural development of the hippocampus and episodic memory: developmental differences along the anterior/posterior axis. Cereb. Cortex 24, 3036–3045.
DeMaster, D.M., Ghetti, S., 2013. Developmental differences in hippocampal and cortical contributions to episodic retrieval. Cortex 49, 1482–1493.
Dolcos, F., Iordan, A.D., Kragel, J., Stokes, J., Campbell, R., McCarthy, G., Cabeza, R., 2013. Neural correlates of opposing effects of emotional distraction on working memory and episodic memory: an event-related FMRI investigation. Front Psychol. 4, 293.
Driscoll, I., 2003. The aging hippocampus: cognitive, biochemical and structural findings. Cereb. Cortex 13, 1344–1351.
Duvernoy, H.M., 2005. Functional anatomy, vascularization and serial sections with MRI. In: The Human Hippocampus. Springer-Verlag, Berlin.

Echavarri, C., Aalten, P., Uylings, H.B., Jacobs, H.I., Visser, P.J., Gronenschild, E.H., Verhey, F.R., Burgmans, S., 2011. Atrophy in the parahippocampal gyrus as an early biomarker of Alzheimer's disease. Brain Struct. Funct. 215, 265–271.
Ekstrom, A.D., Copara, M.S., Isham, E.A., Wang, W.C., Yonelinas, A.P., 2011. Dissociable networks involved in spatial and temporal order source retrieval. Neuroimage 56, 1803–1813.
Eritaia, J., Wood, S.J., Stuart, G.W., Bridle, N., Dudgeon, P., Maruff, P., Velakoulis, D., Pantelis, C., 2000. An optimized method for estimating intracranial volume from magnetic resonance images. Magn. Reson. Med. 44, 973–977.
Fanselow, M.S., Dong, H.W., 2010. Are the dorsal and ventral hippocampus functionally distinct structures? Neuron 65, 7–19.
Gimenez, M., Junque, C., Narberhaus, A., Caldu, X., Salgado-Pineda, P., Bargallo, N., Segarra, D., Botet, F., 2004. Hippocampal gray matter reduction associates with memory deficits in adolescents with history of prematurity. Neuroimage 23, 869–877.
Giovanello, K.S., Schnyer, D., Verfaellie, M., 2009. Distinct hippocampal regions make unique contributions to relational memory. Hippocampus 19, 111–117.
Gogtay, N., Nugent 3rd, T.F., Herman, D.H., Ordonez, A., Greenstein, D., Hayashi, K.M., Clasen, L., Toga, A.W., Giedd, J.N., Rapoport, J.L., Thompson, P.M., 2006. Dynamic mapping of normal human hippocampal development. Hippocampus 16, 664–672.
Gordon, B.A., Blazey, T., Benzinger, T.L., Head, D., 2013. Effects of aging and Alzheimer's disease along the longitudinal axis of the hippocampus. J, Alzheimer's Dis. 37, 41–50.
Hayes, A.F., Scharkow, M., 2013. The relative trustworthiness of inferential tests of the indirect effect in statistical mediation analysis: does method really matter? Psychol. Sci. 24, 1918–1927.
Insausti, R., Cebada-Sanchez, S., Marcos, P., 2010. Postnatal development of the human hippocampal formation. Adv. Anat. Embryol. Cell Biol. 206, 1–86.
Jack Jr., C.R., Twomey, C.K., Zinsmeister, A.R., Sharbrough, F.W., Petersen, R.C., Cascino, G.D., 1989. Anterior temporal lobes and hippocampal formations: normative volumetric measurements from MR images in young adults. Radiology 172, 549–554.
Kalpouzos, G., Chetelat, G., Baron, J.C., Landeau, B., Mevel, K., Godeau, C., Barre, L., Constans, J.M., Viader, F., Eustache, F., Desgranges, B., 2009. Voxel-based mapping of brain gray matter volume and glucose metabolism profiles in normal aging. Neurobiol. Aging 30, 112–124.
Krogsrud, S.K., Tamnes, C.K., Fjell, A.M., Amlien, I., Grydeland, H., Sulutvedt, U., Due-Tonnessen, P., Bjornerud, A., Solsnes, A.E., Haberg, A.K., Skrane, J., Walhovd, K.B., 2014. Development of hippocampal subfield volumes from 4 to 22 years. Hum. Brain Mapp.
Lee, J.K., Ekstrom, A.D., Ghetti, S., 2014. Volume of hippocampal subfields and episodic memory in childhood and adolescence. Neuroimage 94, 162–171.
Lin, M., Fwu, P.T., Buss, C., Davis, E.P., Head, K., Muftuler, L.T., Sandman, C.A., Su, M.Y., 2013. Developmental changes in hippocampal shape among preadolescent children. Int. J. Dev. Neurosci. 31, 473–481.
Lindenberger, U., von Oertzen, T., Ghisletta, P., Hertzog, C., 2011. Cross-sectional age variance extraction: what's change got to do with it? Psychol. Aging 26, 34–47.
Longoni, G., Rocca, M.A., Pagani, E., Riccitelli, G.C., Colombo, B., Rodegher, M., Falini, A., Comi, G., Filippi, M., 2013. Deficits in memory and visuospatial learning correlate with regional hippocampal atrophy in MS. Brain Struct. Funct.
Maguire, E.A., Gadian, D.G., Johnsrude, I.S., Good, C.D., Ashburner, J., Frackowiak, R.S., Frith, C.D., 2000. Navigation-related structural change in the hippocampi of taxi drivers. Proc. Natl. Acad. Sci. U. S. A. 97, 4398–4403.
Maller, J.J., Reglade-Meslin, C., Anstey, K.J., Sachdev, P., 2006. Sex and symmetry differences in hippocampal volumetrics: before and beyond the opening of the crus of the fornix. Hippocampus 16, 80–90.
Malykhin, N.V., Bouchard, T.P., Ogilvie, C.J., Coupland, N.J., Seres, P., Camicioli, R., 2007. Three-dimensional volumetric analysis and reconstruction of amygdala and hippocampal head, body and tail. Psychiatry Res. 155, 155–165.
Malykhin, N.V., Lebel, R.M., Coupland, N.J., Wilman, A.H., Carter, R., 2010. In vivo quantification of hippocampal subfields using 4.7 T fast spin echo imaging. Neuroimage 49, 1224–1230.
Martin, S.B., Smith, C.D., Collins, H.R., Schmitt, F.A., Gold, B.T., 2010. Evidence that volume of anterior medial temporal lobe is reduced in seniors destined for mild cognitive impairment. Neurobiol. Aging 31, 1099–1106.
Mattai, A., Hosanagar, A., Weisinger, B., Greenstein, D., Stidd, R., Clasen, L., Lalonde, F., Rapoport, J., Gogtay, N., 2011. Hippocampal volume development in healthy siblings of childhood-onset schizophrenia patients. Am. J. Psychiatry 168, 427–435.
Morgan, L.K., Macevoy, S.P., Aguirre, G.K., Epstein, R.A., 2011. Distances between real-world locations are represented in the human hippocampus. J. Neurosci. 31, 1238–1245.
Moser, M.B., Moser, E.I., 1998. Functional differentiation in the hippocampus. Hippocampus 8, 608–619.
Murty, V.P., Ritchey, M., Adcock, R.A., LaBar, K.S., 2010. fMRI studies of successful emotional memory encoding: a quantitative meta-analysis. Neuropsychologia 48, 3459–3469.
Pluta, J., Yushkevich, P., Das, S., Wolk, D., 2012. In vivo analysis of hippocampal subfield atrophy in mild cognitive impairment via semi-automatic segmentation of T2-weighted MRI. J. Alzheimer's Dis. 31, 85–99.
Poppenk, J., Evensmoen, H.R., Moscovitch, M., Nadel, L., 2013. Long-axis specialization of the human hippocampus. Trends Cognit. Sci. 17, 230–240.
Poppenk, J., Moscovitch, M., 2011. A hippocampal marker of recollection memory ability among healthy young adults: contributions of posterior and anterior segments. Neuron 72, 931–937.
Pruessner, J.C., Collins, D.L., Pruessner, M., Evans, A.C., 2001. Age and gender predict volume decline in the anterior and posterior hippocampus in early adulthood. J. Neurosci. 21, 194–200.
Qiu, L.R., Germann, J., Spring, S., Alm, C., Vousden, D.A., Palmert, M.R., Lerch, J.P., 2013. Hippocampal volumes differ across the mouse estrous cycle, can change within 24 hours, and associate with cognitive strategies. Neuroimage 83, 593–598.
Raz, N., Rodrigue, K.M., Head, D., Kennedy, K.M., Acker, J.D., 2004. Differential aging of the medial temporal lobe: a study of a five-year change. Neurology 62, 433–438.
Ryan, L., Lin, C.Y., Ketcham, K., Nadel, L., 2010. The role of medial temporal lobe in retrieving spatial and nonspatial relations from episodic and semantic memory. Hippocampus 20, 11–18.
Schneider, J.F., Vergesslich, K., 2007. Maturation of the limbic system revealed by MR FLAIR imaging. Pediatr. Radiol. 37, 351–355.
Scoville, W.B., Milner, B., 1957. Loss of recent memory after bilateral hippocampal lesions. J. Neurol. Neurosurg. Psychiatry 20, 11–21.
Sgouros, S., Natarajan, K., Hockley, A.D., Goldin, J.H., Wake, M., 1999. Skull base growth in childhood. Pediatr. Neurosurg. 31, 259–268.
Shafer, A.T., Dolcos, F., 2012. Neural correlates of opposing effects of emotional distraction on perception and episodic memory: an event-related FMRI investigation. Front. Integr. Neurosci. 6, 70.
Shrout, P.E., Fleiss, J.L., 1979. Intraclass correlations: uses in assessing rater reliability. Psychol. Bull. 86, 420–428.
Strange, B.A., Witter, M.P., Lein, E.S., Moser, E.I., 2014. Functional organization of the hippocampal longitudinal axis. Nat. Rev. Neurosci. 15, 655–669.
Sullivan, E.V., Pfefferbaum, A., Rohlfing, T., Baker, F.C., Padilla, M.L., Colrain, I.M., 2011. Developmental change in regional brain structure over 7 months in early adolescence: comparison of approaches for longitudinal atlas-based parcellation. Neuroimage 57, 214–224.
Tamnes, C.K., Walhovd, K.B., Engvig, A., Grydeland, H., Krogsrud, S.K., Ostby, Y., Holland, D., Dale, A.M., Fjell, A.M., 2014. Regional hippocampal volumes and development predict learning and memory. Dev. Neurosci. 36, 161–174.
Tulving, E., Markowitsch, H.J., 1998. Episodic and declarative memory: role of the hippocampus. Hippocampus 8, 198–204.
Watson, C., Jack Jr., C.R., Cendes, F., 1997. Volumetric magnetic resonance imaging: Clinical applications and contributions to the understanding of temporal lobe epilepsy. Arch. Neurol. 54, 1521–1531.
Weiss, A.P., Dewitt, I., Goff, D., Ditman, T., Heckers, S., 2005. Anterior and posterior hippocampal volumes in schizophrenia. Schizophrenia Res. 73, 103–112.
Wenger, E., Martensson, J., Noack, H., Bodammer, N.C., Kuhn, S., Schaefer, S., Heinze, H.J., Duzel, E., Backman, L., Lindenberger, U., Lovden, M., 2014. Comparing manual and automatic segmentation of hippocampal volumes: reliability and validity issues in younger and older brains. Hum. Brain Mapp. 35, 4236–4248.
Widjaja, E., Zamyadi, M., Raybaud, C., Snead, O.C., Smith, M.L., 2014. Volumetric changes in hippocampal subregions and their relation to memory in pediatric nonlesional localization-related epilepsy. Epilepsia 55, 519–527.
Woollett, K., Maguire, E.A., 2012. Exploring anterograde associative memory in London taxi drivers. Neuroreport 23, 885–888.
Yushkevich, P.A., Wang, H., Pluta, J., Das, S.R., Craige, C., Avants, B.B., Weiner, M.W., Mueller, S., 2010. Nearly automatic segmentation of hippocampal subfields in in vivo focal T2-weighted MRI. Neuroimage 53, 1208–1224.